Investigation on the relationship between overpressure and sub-harmonic response from encapsulated microbubbles*

Wu Jun(吴 军)[a], Fan Ting-Bo(范庭波)[b)c)], Xu Di(许 迪)[a)†], and Zhang Dong(章 东)[c)‡]

[a)] *The First Affiliated Hospital of Nanjing Medical University, Nanjing* 210029, *China*
[b)] *Jiangsu Provincial Institute for Medical Equipment Testing, Nanjing* 210012, *China*
[c)] *Institute of Acoustics, Key Laboratory of Modern Acoustics, Ministry of Education, Nanjing University, Nanjing* 210093, *China*

(Received 24 November 2013; revised manuscript received 2 March 2014; published online 10 August 2014)

Sub-harmonic component generated from microbubbles is proven to be potentially used in noninvasive blood pressure measurement. Both theoretical and experimental studies are performed in the present work to investigate the dependence of the sub-harmonic generation on the overpressure with different excitation pressure amplitudes and pulse lengths. With 4-MHz ultrasound excitation at an applied acoustic pressure amplitude of 0.24 MPa, the measured sub-harmonic amplitude exhibits a decreasing change as overpressure increases; while non-monotonic change is observed for the applied acoustic pressures of 0.36 MPa and 0.48 MPa, and the peak position in the curve of the sub-harmonic response versus the overpressure shifts toward higher overpressure as the excitation pressure amplitude increases. Furthermore, the exciting pulse with long duration could lead to a better sensitivity of the sub-harmonic response to overpressure. The measured results are explained by the numerical simulations based on the Marmottant model. The numerical simulations qualitatively accord with the measured results. This work might provide a preliminary proof for the optimization of the noninvasive blood pressure measurement through using sub-harmonic generation from microbubbles.

Keywords: microbubble, overpressure, sub-harmonic response, blood pressure measurement

PACS: 43.25.+y, 43.80.+p **DOI:** 10.1088/1674-1056/23/10/104302

1. Introduction

Pulmonary hypertension (PH) refers to high blood pressure in the vessel that carries blood from the heart to the lungs.[1] Since the symptoms of PH are not specific, accurate diagnosis of PH is still a great obstacle facing the researchers and clinicians, although many tests might give clues to the possibility of PH. For instance, the right heart catheterization (RHC) is currently considered as the best diagnostic modality of PH.[1] However, this technique is invasive and subject to the high risk of patients' infection. Therefore, exploration of more safe and accurate diagnostic methods is always in high demand for improving PH treatment.

Ultrasound contrast agent (UCA) is usually comprised of suspensions of gas-filled microbubbles with micrometer diameters encapsulated by a thin stabilization coating (e.g., lipid, albumin, or polymer).[2,3] UCAs were initially used in ultrasound medical applications to enhance acoustic contrast between blood and surrounding tissues and thereby to improve the quality of ultrasonic images. Besides enhancing the reflection of ultrasound, the UCA microbubbles also exhibit nonlinear vibrations under insonation, which will produce harmonic, sub-harmonic, and ultra-harmonic responses.[4,5] In the past several decades, various methods have been proposed for non-invasive blood pressure measurements using UCA microbubbles. Fairbank and Scully developed a modality for cardiac pressure measurements by using the resonant frequency of UCAs.[6] Bouakaz *et al.* proposed an approach to blood pressure measurement based on the measurement of the disappearance time of free bubbles.[7] Recently, sub-harmonic response has been proposed as a possible modality for local blood pressure measurement, owing to approximately linear reduction in sub-harmonic response as overpressure increases.[8] Shi *et al.*[9] and Leodore *et al.*[10] experimentally found that the sub-harmonic response from UCA microbubbles is robustly dependent on the overpressure. However, the sub-harmonic responses of UCAs might exhibit different tendencies as the overpressure increases at different excitation levels. Frinking *et al.* revealed that the sub-harmonic response might increase by 28.9 dB for 180-mm Hg increase of overpressure at a low excitation level of 50 kPa; while the sub-harmonic response exhibited a 9.6-dB decrease at a higher excitation pressure of 400 kPa.[11] Andersen and Jensen theoretically proved that the variation of sub-harmonic component should be related to the exciting parameters, such as the pulse shape, length, and amplitude.[12] Katiyar *et al.* revealed that the change in the sub-harmonic response might be dominated by the ratio of the

*Project supported by the National Basic Research Program from Ministry of Science and Technology, China (Grant No. 2011CB707900), the National Natural Science Foundation of China (Grant Nos. 81271589, 81227004, 11174141, 11374155, 11612032, and 81301616), and the Natural Science Foundation of Jiangsu Province, China (Grant Nos. BE2011110 and BK20131017).

†Corresponding author. E-mail: di_hsu@126.com
‡Corresponding author. E-mail: dzhang@nju.edu.cn

© 2014 Chinese Physical Society and IOP Publishing Ltd

excitation frequency to the natural frequency of the bubble.[13]

In the present study, the relationship between overpressure and sub-harmonic generation under different ultrasonic excitation conditions (viz. amplitude and pulse length) is further experimentally examined. Moreover, numerical simulations based on the Marmottant model[14] are performed to explain the measured results. This work is helpful for optimizing the noninvasive blood pressure measurement by making use of the sub-harmonic response generated from UCA microbubbles.

2. Theory and method

Microbubble dynamics in an incompressible liquid has been studied widely using various types of modified Rayleigh–Plesset (RP) equations.[14] In the present study, the Marmottant model is used for describing the dynamic behavior of microbubbles encapsulated with thin lipid shell.[14] The dynamic equation of the model is written as

$$\begin{aligned}&\rho R\ddot{R}+\frac{3}{2}\rho\dot{R}^2\\&=\left[P_0+P_{\rm ov}+\frac{2\sigma(R_0)}{R_0}\right]\left(\frac{R_0}{R}\right)^{3\kappa}\left(1-\frac{3\kappa}{c}\dot{R}\right)\\&\quad-(P_0+P_{\rm ov})-\frac{2\sigma(R)}{R}-\frac{4\mu\dot{R}}{R}-\frac{4\kappa_{\rm s}\dot{R}}{R^2}-p_{\rm ac}(t),\end{aligned}\quad(1)$$

where R is the instantaneous radius of the microbubble; $\dot{R}$ and $\ddot{R}$ are the first and second time derivatives of R; R_0 is the equilibrium radius; ρ is the density of the surrounding medium; κ is the polytropic exponent; μ is the surrounding liquid viscosity; $\kappa_{\rm s}$ is the surface dilatational viscosity; P_0 is the hydrostatic pressure; $P_{\rm ov}$ is the overpressure (to evaluate the variation of ambient pressure); $P_{\rm ac}(t)$ is the exciting acoustic pressure; c is the sound velocity. The Marmottant model underlines the effective surface tension of a microbubble during its oscillation, and the movement of the bubble is defined as three successive stages as the surface tension rises. The effective surface tension $\sigma(R)$ is expressed as[14]

$$\sigma(R)=\begin{cases}0, & \text{if } R\le R_{\rm buckling},\\ \chi\left(\dfrac{R^2}{R_{\rm buckling}^2}-1\right), & \text{if } R_{\rm buckling}\le R\le R_{\rm break-up},\\ \sigma_{\rm water}, & \text{if ruptured and } R\ge R_{\rm ruptured}.\end{cases}\quad(2)$$

In this model, three parameters describe the properties of the shell: a buckling radius, the compressibility of the shell, and a break-up shell tension. In the buckling state where the bubble radius is below the buckling radius $R_{\rm buckling}$, the surface tension is assumed to nearly vanish, i.e., $\sigma=0$. The shell is elastic only in a narrow region where the lower limit radius is $R_{\rm buckling}$, while the upper limit radius is fixed by the maximum surface tension, which is $\sigma_{\rm water}$ after rupture, giving $R_{\rm ruptured}=R_{\rm buckling}(1+\sigma_{\rm water}/\chi)^{1/2}$. The value of the elastic modulus can hold true for the presence of any solid-like shell material that sustains tensile stress. A constant elastic modulus χ is assigned in this state. Within this region the surface tension is a linear function of the square of the radius. Finally, after break-up, the surface tension is assumed to relax to $\sigma_{\rm water}$.

The scattered acoustic response is calculated from the radial response at a distance of d from the microbubble as follows:[15]

$$P_{\rm s}(d,t)=\rho\frac{R}{d}(2\dot{R}^2+R\ddot{R}).\quad(3)$$

Considering the fact that UCA microbubbles have a wide size distribution, a weighting scheme[15,16] is utilized to determine the cumulative echoes on the basis of the size distribution of microbubbles. $S(f)$ represents the total scattered pressure from microbubbles with sizes ranging from R_i to R_j at a frequency f, and it is expressed as

$$S(f)=\sum_{k=i}^{j}P_{\rm SC}(R_k,f)w_k\%,\quad(4)$$

where $P_{\rm SC}(R_k,f)$ is the scattered pressure from microbubbles with size R_k at frequency f, and w_k is the number percentage weight of bubbles with size R_k.

On the other hand, note that the linear resonance frequency f_0 of a microbubble is

$$f_0=\frac{1}{2\pi R_0}\sqrt{\frac{1}{\rho}\left[3\kappa P_{\rm amp}+\frac{2\sigma(R_0)}{R_0}(3\kappa-1)\right]},\quad(5)$$

where $P_{\rm amp}=P_0+P_{\rm ov}$. It is noted that the resonance frequency depends both on ambient pressure and on radius. For simplicity, in the calculation of the resonance frequency of the microbubble clouds, the average radius is used.

In the simulation, some physical constants are set as listed in Table 1.[17]

Table 1. Parameters of microbubbles.

Symbol	Description	Value
$\kappa_{\rm s}$	shell surface dilatational viscosity	1.66×10^{-7} kg/s
χ	shell elastic compression modulus	1.05 N/m
σ_0	surface tension in the equilibrium	0.25 N/m
$\sigma_{\rm break-up}$	critical tension where shell breaks	0.13 N/m
$d_{\rm s}$	shell thickness of bubble (m)	$0.1\%\times R_0$
$\sigma_{\rm water}$	water surface tension	0.072 N/m
p_0	hydrostatic pressure	1.01×10^5 N/m^2
κ	polytropic exponent of the gas	1.4
ρ	density of surrounding liquid	998 Kg/m^3
c	sound speed in liquid	1500 m/s
μ	viscous in liquid	1.0×10^{-3} N·s/m^2
R_0	equilibrium radius	2.0 μm
$R_{\rm buckling}$	shell buckling radius	1.8 μm
κ	polytropic exponent	1.07

3. Experimental setup

The encapsulated microbubbles were prepared according to the following steps: (i) distearoyl phosphatidylcholine (DSPC), dipalmitoylphosphoglycerol (DPPG), and polyethylene glycol (PEG) were mixed and dissolved in the degassed water; (ii) the solution was then put into a 1-ml penicillin vial and then frozen and desiccated at -20 °C; (iii) a solution containing glycerin and propylene glycol was added into the vial and saturated with C_3F_8 gas; (iv) after 45-second mechanical shaking, the bubble solution was ready and then diluted to a concentration of around 2.0×10^6 microbubbles/ml for experimental use. The average radius of the encapsulated microbubbles is around 2 μm (corresponding to the peak in the microbubble distribution). Based on Eq. (5), the resonance frequency is about 2.4 MHz. The size distribution of microbubbles was measured by a Coulter Counter (Coulter Corporation, Hialeah, FL) as shown in Fig. 1. The elasticity of the shell was determined by the optimization method based on the sound attenuation spectrum.[18,19] The determined parameters for microbubbles are listed in Table 1.

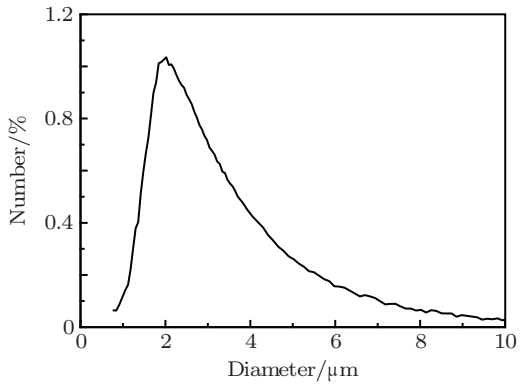


Fig. 1. Size distribution of microbubbles.

Figure 2 shows the diagram of the experimental setup for measuring the sub-harmonics responses scattered from UCA microbubbles. An arbitrary waveform generator (Agilent 33250, CA, USA) was used to produce 4-MHz tone-burst signals with different pulse lengths (16, 32 or 64 cycles) at a pulse repetitive frequency (PRF) of 100 Hz. After being amplified by an RF power amplifier (A150, ENI, Rochester, NY, USA), the signals were used to drive a plane transducer (V382-SU, Panametrics, MA, central frequency = 4.0 MHz, diameter = 1 cm). The scattered wave was received by another plane transducer (V382-SU, Panametrics, MA, central frequency = 2.25 MHz, diameter = 1 cm). After passing through a pre-amplifier (fixed gain of 30 dB, HPA30, NTR Systems, Inc. Seattle, WA, USA), the received signal was captured by a digital oscilloscope (Agilent 54810, Santa Clara, CA, USA). The transmitter and receiver were orthogonally located in order to reduce the influence of the insonating signal on the detection of the sub-harmonic signals. A plastic transparent pipe with 6.0-mm outer diameter and 5.0-mm inner diameter was used to hold the microbubble suspension. One end of the pipe was airtight, and the other end was connected with a syringe containing 50-ml air. The overpressure was controlled by changing the air volume in the syringe. A linear 3-axial scanning system (ESP7000, Newport, USA) controlled by a PC via a Labview software (NI Corp., TX) was used for aligning the transmitter and receiver. The *in situ* acoustic pressure of the transmitting transducer was calibrated by using a needle hydrophone (TNU001A, NTR Systems, Inc. Seattle, WA) with a 30-dB preamplifier (HPA30, NTR Systems, Inc. Seattle, WA, USA). All measurements were performed at room temperature (approximately 23 °C). Five replicated measurements were performed at each setting for the sub-harmonic emissions with refreshed microbubble suspensions. For each measurement, the responses of microbubbles were averaged over 100 traces and then analyzed by using a fast-Fourier-transform (FFT) program.

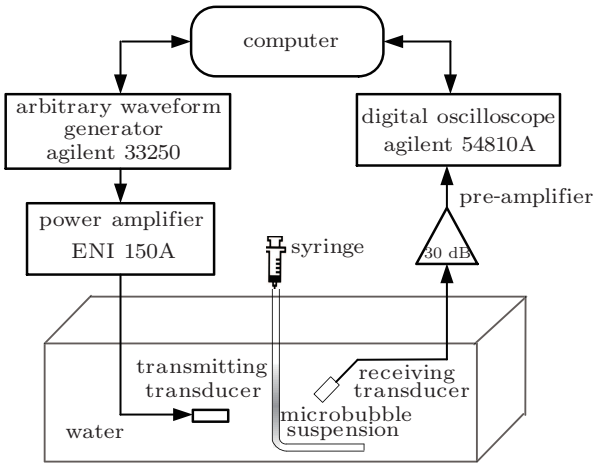


Fig. 2. Experiment setup for measuring sub-harmonic response from microbubbles.

4. Results and discussion

It has been reported that the generation of sub-harmonics occurs when the exciting acoustic pressure exceeds a certain threshold, and the threshold pressure reaches a minimum level at $f = 2f_0$.[18] Figure 3 shows the measured attenuation spectrum for the microbubbles. It is seen that the resonant frequency of the microbubbles is around 2.4 MHz. Considering the available transducers in our laboratory, the exciting frequency of 4 MHz is chosen in both the simulations and the measurements. Figure 4(a) shows the spectrum of the signal scattered from microbubbles excited by 4-MHz ultrasound at an acoustic pressure of 0.36 MPa and pulse length of 64 cycles, where the curve is normalized to the sub-harmonic amplitude. Significant discrete sub-harmonic component is observed, which indicates that this frequency can be utilized to generate sufficient sub-harmonic signal. Figure 4(b) shows

the amplitude of sub-harmonic component versus driven pressure in a range from 0.05 MPa to 0.75 MPa with an overpressure of 14 kPa. It is shown that the pressure threshold for the generation of sub-harmonic response is about 0.12 MPa. When the exciting acoustic pressure increases from 0.15 MPa to 0.5 MPa, the amplitude of the sub-harmonic component is enhanced by 28 dB. The sub-harmonic amplitude reaches saturation as the exciting acoustic pressure exceeds 0.5 MPa. The result indicates that the sub-harmonic responses generated from microbubbles can be divided into three stages, i.e. generation, rapid rise, and saturation, which coincides well with the reported results.[18,19] In the following experiments, microbubbles will be driven by ultrasound pulses at pressures of 0.24, 0.36, and 0.48 MPa, respectively.

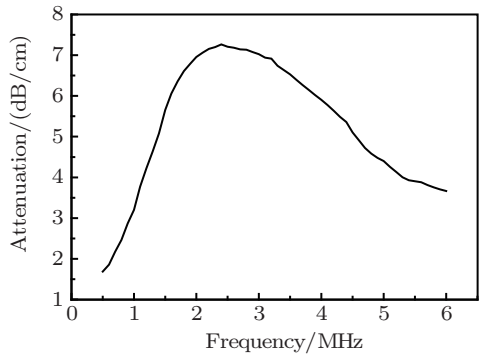


Fig. 3. Attenuation spectrum of the microbubbles.

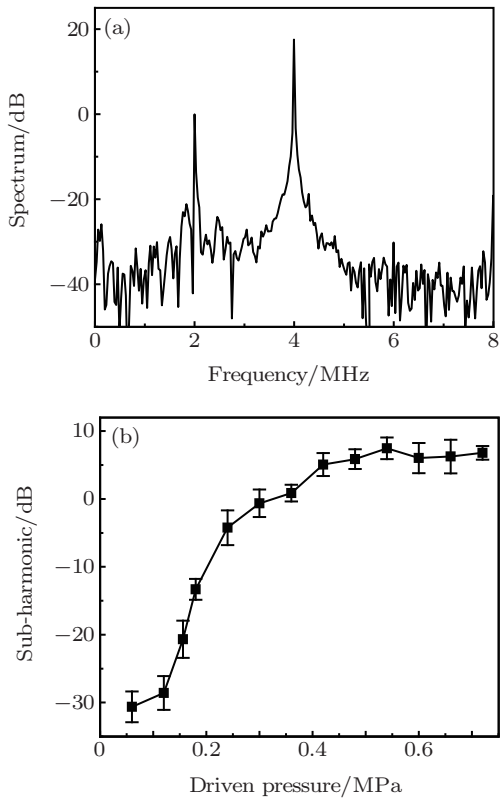


Fig. 4. (a) Spectrum of the scattered signal from microbubbles, and (b) sub-harmonic versus exciting acoustic pressure.

Figure 5 shows the dependences of sub-harmonic response on overpressure at different exciting acoustic pressure amplitudes (Fig. 5(a)) and pulse lengths (Fig. 5(b)). In Fig. 5(a), the pulse length is fixed to be 64 cycles, and the excitation pressure is kept at 0.36 MPa in Fig. 5(b). As shown in Fig. 5(a), the sub-harmonic amplitude shows a decreasing change of the sub-harmonic amplitude as the overpressure increases for the applied acoustic pressure amplitude of 0.24 MPa. However, non-monotonic changes are observed for the applied acoustic pressures of 0.36 MPa and 0.48 MPa. There is an increasing tendency as the overpressure increases at the initial stage; after reaching a peak, the sub-harmonic amplitude begins to decrease with the increasing of overpressure. In addition, the position of maximum sub-harmonic amplitude shifts toward higher overpressure for higher excitation acoustic pressure. The maximum sub-harmonic amplitudes occur at overpressures of 8.8 kPa and 13.8 kPa corresponding to the exciting acoustic pressures of 0.36 MPa and 0.48 MPa respectively. Previous studies have indicated that the sub-harmonic amplitude increases or decreases monotonically with the increasing of overpressure.[10–12] The non-monotonic variation of sub-harmonic in the present study is related to the change of the resonance frequency of UCA microbubbles, which will be discussed later.

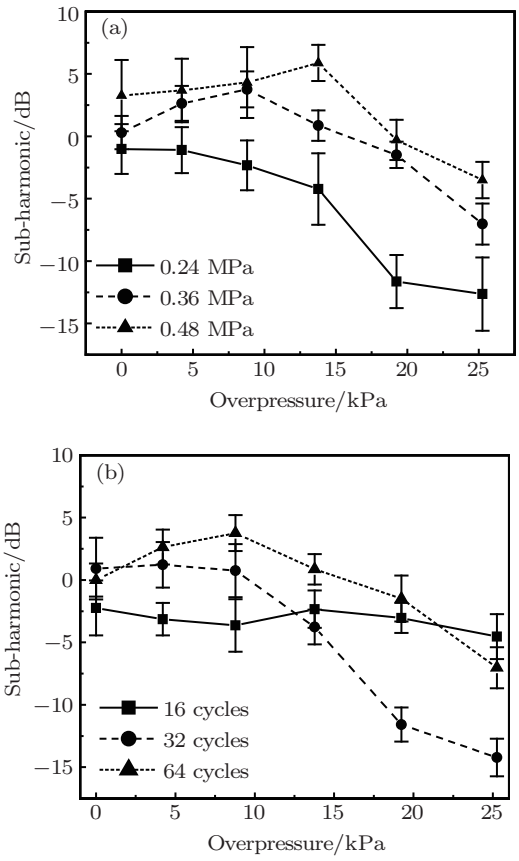


Fig. 5. Dependences of sub-harmonic amplitude on overpressure for different (a) exciting acoustic pressures and (b) pulse lengths.

When the exciting acoustic pressure amplitude is kept at 0.36 MPa, the dependences of the sub-harmonic response on the overpressure for different pulse lengths are shown in Fig. 5(b). It is observed that the sub-harmonic amplitude increases as the pulse length increases from 32 cycles to 64 cycles. However, for the pulse length of 16 cycles, the sub-harmonic amplitude almost keeps constant when the overpressure changes from 0 to 25 kPa. It indicates that for the ultrasound exposure with a pulse length of 16 cycles, the sensitivity of the sub-harmonic component to the variation of ambient pressure is too low, owing to the reduction of the ultrasonic energy.

Figure 6(a) shows the curve of calculated amplitude of sub-harmonics versus applied acoustic pressure with overpressure of 14 kPa. With exciting acoustic pressure increasing from 0.1 MPa to 0.42 MPa, the sub-harmonic amplitude increases by 47 dB. The sub-harmonic amplitude reaches saturation when the driving pressure exceeds 0.36 MPa. Compared with the measured results (Fig. 4(b)), the change tendency is almost the same, but the excitation pressure at which the sub-harmonics is saturated is much lower than the measured one. The possible reason is that the microbubble model used in the simulation takes no account of the microbubble destruction.

The amplitudes of sub-harmonics are calculated each as a function of exciting frequency at zero overpressure and three exciting pressure levels (viz. 0.24, 0.36, and 0.48 MPa). The calculated results are demonstrated in Fig. 6(b), where the exciting frequency is normalized by the resonance frequency (calculated from the averaged radius). It is obvious that similar variation tendencies can be observed at different exciting pressure levels. For example, when the exciting acoustic pressure amplitude is 0.36 MPa, the sub-harmonic response initially increases as $f/f_0 \leq 1.64$. Then, the sub-harmonic amplitude reaches a peak value at $f/f_0 = 1.64$. Non-smooth variation is observed for the sub-harmonic amplitudes when $1.64 \leq f/f_0 \leq 1.82$, while the sub-harmonic amplitude decreases monotonically for $f/f_0 > 1.82$. As indicated by Eq. (5), if the overpressure increases, the microbubble resonance frequency increases, leading to the reduction of f/f_0. Consequently, if the exciting frequency satisfies the inequality $f/f_0 \leq 1.64$, the sub-harmonic amplitude will decrease with the increasing of the overpressure; inversely, if the exciting frequency satisfies the inequality $f/f_0 \geq 1.82$, the sub-harmonic amplitude will increase with the increasing of overpressure. While for $1.64 \leq f/f_0 \leq 1.82$, the curve of the sub-harmonic amplitude versus overpressure is non-monotonic. These results may provide a likely explanation for the measured change of the sub-harmonic response with overpressure. In addition, one can find in Fig. 6(b) that the peak positions of the sub-harmonic amplitudes shift toward the lower values of f/f_0 as the exciting pressure increases. The simulated results are also in agreement with the measured curves in Fig. 5(a), where the peaks of the sub-harmonic amplitudes occur at 8.8 kPa and 13.8 kPa corresponding to the exciting acoustic pressures of 0.36 MPa and 0.48 MPa. It should be noted that the resonance frequency can be affected by the microbubble size distribution and the overpressure change. For simplicity, in the calculations of Fig. 6(b), these effects are not considered and only the average microbubble radius is used in the calculation.

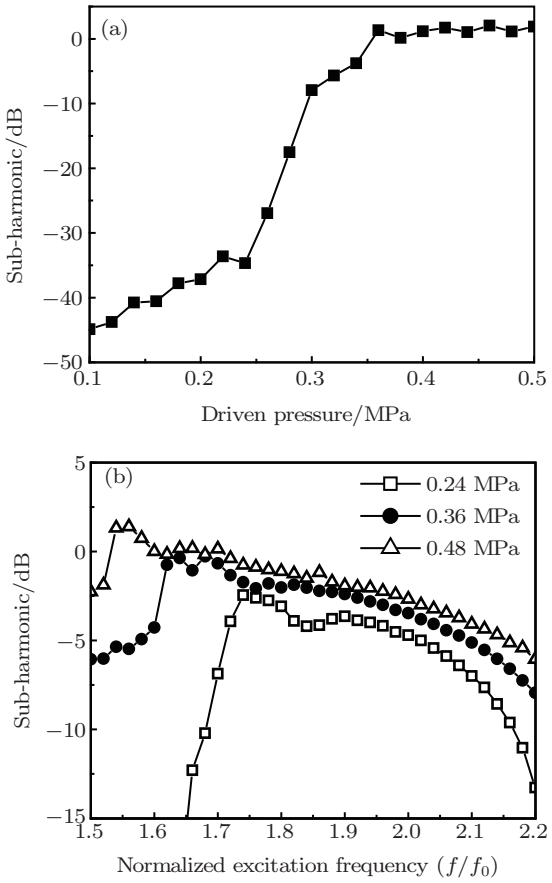


Fig. 6. Calculated sub-harmonic responses as a function of (a) exciting pressure amplitude, and (b) exciting frequency.

Figure 7 shows the curves of calculated sub-harmonic response versus overpressure when the microbubble is driven by 4-MHz ultrasonic pulses with different pressure amplitudes and pulse lengths. In Fig. 7(a), the exciting pulse length is fixed at 64 cycles. For an excitation pressure amplitude of 0.24 MPa, the sub-harmonic amplitude decreases with the increasing of overpressure. However, for an exciting pressure amplitude of 0.48 MPa, the change of sub-harmonic amplitude becomes non-monotonic. In this study, the driving frequency is 4 MHz, the corresponding f/f_0 is 1.69. As indicated by the curve at 0.24 MPa in Fig. 6(b), the sub-harmonic amplitude decreases with the increasing of the overpressure for $f/f_0 < 1.74$. Compared with the measured results shown in Fig. 5(a), the sub-harmonic amplitude shows decreasing tendency only for 0.24 MPa, which is in agreement with the simulated results.

Figure 7(b) shows the influence of the pulse length on the sub-harmonic response when the microbubble is driven at an acoustic pressure of 0.36 MPa. With the increasing of pulse length, the sub-harmonic response becomes more sensitive to the overpressure. For an excitation pulse of 16 cycles, the sub-harmonic amplitude decreases by 12 dB when the overpressure changes from 0 kPa to 25 kPa. By contrast, for a pulse of 64 cycles, the sub-harmonic amplitude decreases by about 28 dB. It indicates that the pulse with longer pulse length will lead to a better sensitivity for the overpressure measurement.

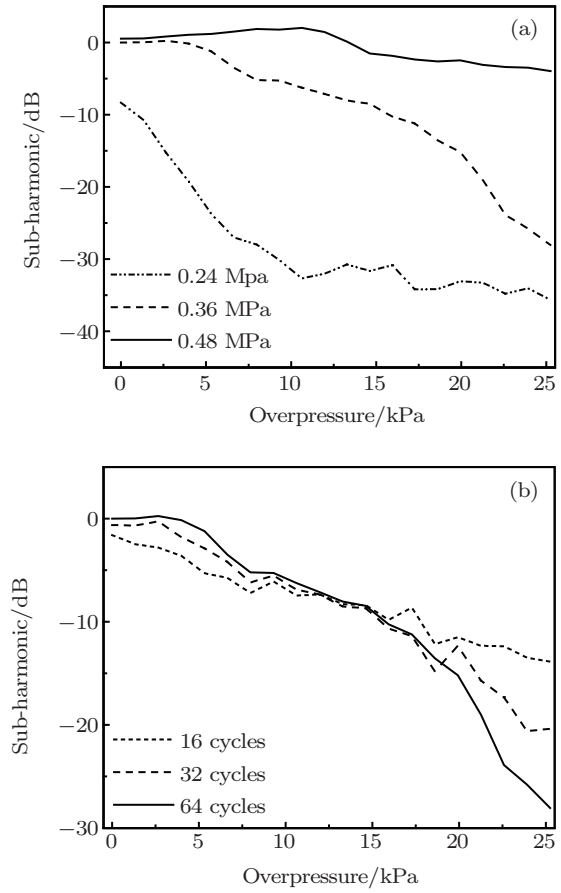


Fig. 7. Calculated dependences of sub-harmonic amplitude on the overpressure for different (a) exciting acoustic pressure amplitudes, and (b) pulse lengths.

Previous studies have indicated that the non-invasive blood pressure measurement could be made based on either the increasing or the decreasing of the sub-harmonic generation from UCA microbubbles.[11,12] In the present work, it is noticed that the relationship between the sub-harmonic generation and the overpressure shows either decreasing or non-monotonic change. The relation mainly depends on the ratio of the exciting frequency to the resonant frequency, i.e., f/f_0, the exciting acoustic pressure amplitude, and the microbubble parameters. For the UCA microbubbles used in this study, the monotonic change can be derived at 4-MHz ultrasound excitation with an acoustic pressure of 0.24 MPa. When increasing the acoustic pressure, the relation will become non-monotonic. The results confirm the theoretical results obtained by Katiyar.[13] If choosing the exciting frequency close to $2f_0$, the effect of the acoustic pressure amplitude on the monotonic relationship can be reduced as indicated by Fig. 6(b).

Note that the variation of sub-harmonic component in the numerical simulations is more significant than the measured result. The main reason is that the model used in this study takes no account of the microbubble interactions and the variations of the shell parameters as the radius changes. In addition, in the discussion of the effect of f/f_0 on the generation of the sub-harmonics, microbubble size distribution is not considered, and the resonance frequency f_0 is calculated with the averaged radius. However, the simulated results still can provide qualitative interpretation for the experimental results. This implies that the ultrasound exciting conditions can be optimized based on this theoretical model, and it may suggest that the sensitivity achievable for noninvasive pressure measurement can be improved further by carefully tuning the microbubble parameters. This may require a contrast agent specifically designed for noninvasive pressure measurements, which will be the object of future studies.

5. Conclusion

In this paper, the dependence of the sub-harmonic amplitude of microbubbles on the overpressure is investigated under different acoustic driving conditions by both experimental measurements and numerical simulations. In the experiments, either decreasing or non-monotonic curves of the sub-harmonic amplitude versus overpressure are measured. The ratio of exciting frequency to microbubble resonance frequency and the acoustic pressure amplitude are shown to be the dominant parameters that can determine the change tendency of the sub-harmonics. The results also demonstrate that the exciting signal with longer pulse length could provide a better sensitivity of the sub-harmonics to the overpressure. This study might provide a foundation for optimizing the local blood pressure measurement through using the sub-harmonic response generated from the microbubbles.

References

[1] Benisty J I 2002 *Circulation* **106** 192
[2] Zhang C B, Liu Z, Guo X S and Zhang D 2010 *Chin. Phys. B* **20** 024301
[3] Huang B, Zhang Y L, Zhang D and Gong X F 2010 *Chin. Phys. B* **19** 054302
[4] de Jong N, Corner R and Lance C T 1994 *Ultrasonics* **32** 447
[5] Shi W T and Forsberg F 2000 *Ultrasound Med. Biol.* **26** 93
[6] Fairbank W M and Scully M O 1977 *IEEE Trans. Biomed. Eng.* **24** 107
[7] Bouakaz A, Frinking P J A, de Jong N and Bom N 1999 *Ultrasound Med. Biol.* **25** 1407

[8] Forsberg F, Liu J B, Shi W T, Furuse J, Shimizu M and Goldberg B B 2005 *IEEE Trans. Ultrason. Ferroelectr. Freq. Control* **52** 581

[9] Shi W T, Forsberg F, Raichlen J S, Needleman L and Goldberg B B 1999 *Ultrasound Med. Biol.* **25** 275

[10] Leodore L M, Forsberg F and Shi W T 2007 *IEEE International Ultrasonics Symposium Proceedings*, P5B-6

[11] Frinking P J A, Gaud E, Brochot J and Arditi M 2010 *IEEE Trans. Ultrason. Ferroelectr. Freq. Control* **57** 1762

[12] Andersen K S and Jensen J A 2009 *J. Acoust. Soc. Am.* **126** 3350

[13] Katiyar A, Sarkar K and Forsberg F 2011 *J. Acoust. Soc. Am.* **129** 2325

[14] Marmottant P, van der Meer S, Emmer M and Versluis M 2005 *J. Acoust. Soc. Am.* **118** 3499

[15] Zheng H R, Barker A and Shandas R 2006 *IEEE Trans. Ultrason. Ferroelectr. Freq. Control* **53** 639

[16] Tang M X, Loughran J, Stride E, Zhang D and Eckersley R J 2011 *J. Acoust. Soc. Am.* **129** EL76

[17] de Jong N, Emmer M, Chin C T, Bouskaz A, Mastik F, Lohse D and Versluis M 2007 *Ultrasound Med. Biol.* **37** 653

[18] Yu J F, Zhang D and Gong X F 2005 *Chin. Phys. Lett.* **22** 892

[19] Gong Y J, Zhang D and Gong X F 2005 *Chin. Sci. Bull.* **50** 1975